

Mini review

Recent progress in electrochemical biosensors for the detection of alpha-fetoprotein as the biomarker of liver cancer

Qiongyu Zhang and Lingbin Ou*

School of Medical Technology, Yongzhou Vocational Technical College, Yongzhou 425100, Hunan, China

*E-mail: qiongyuzhang2009@163.com

Received: 1 March 2022 / *Accepted:* 22 April 2022 / *Published:* 6 June 2022

Alpha fetoprotein (AFP) is one of the clinical tumor biomarkers commonly used in the diagnosis of primary liver cancer. Electrochemical biosensor has the advantages of high analysis speed, low cost and high sensitivity. It is usually used to analyze and detect various cancer markers. In recent years, many electrochemical biosensors for AFP detection have been reported, which made an important contribution to the diagnosis of primary liver cancer. This paper reviews the latest progress of electrochemical biosensors for the detection of AFP as the biomarker of liver cancer.

Keywords: Electrochemical biosensors; alpha-fetoprotein; liver cancer; biomarkers

1. INTRODUCTION

Primary liver carcinoma (PLC) is a common malignant gastrointestinal tumor. The incidence of PLC has been increasing worldwide due to environmental pollution, unhealthy lifestyles, and other factors. PLC is characterized by rapid disease progression, high malignancy, strong invasiveness and poor prognosis. However, there are no obvious symptoms for PLC patients at the early stage. Thus, the treatment effect is poor and the mortality rate is high when the PLC patients are diagnosed. For this view, early diagnosis and treatment of PLC can effectively improve the survival rate of patients. Alpha-fetoprotein (AFP) is one of the commonly used clinical tumor biomarkers for the diagnosis of primary liver cancer [1]. It is a glycoprotein mainly synthesized by fetal liver cells and yolk sac. The concentration of AFP in serum is high at birth, but it will drop to a lower level after one year old. AFP in normal human serum is generally lower than 20 ng/ml. However, when liver cells are damaged, the content of AFP will increase significantly and even exceed 400 ng/mL, especially in the serum of PLC patient. Therefore, the detection of AFP in human serum is of great significance for the early diagnosis

and treatment of PLC.

Currently, various immunological assays have been used to detect AFP in serum. For example, enzyme-linked immunosorbent assay (ELISA), chemiluminescence immunoassay, mass spectrometry, imaging, etc [1]. However, these methods also suffer from some limitations, such as high cost, trained technician, long analysis time, and narrow dynamic range. The analysis of biomarkers by electrochemical technique greatly solves the above problems. Electrochemical biosensors have the advantages of rapid analysis, low cost, and high sensitivity. It has been used for the analysis and detection of various cancer markers [2]. By using nanomaterials, such as gold nanoparticles, graphene, metal-organic frameworks, etc., the compatibility and detection sensitivity of biomarkers can be remarkably improved. In recent years, many electrochemical biosensing platforms for AFP detection have been reported, making important contributions to the diagnosis of primary liver cancer. Herein, we summarized the development of AFP electrochemical biosensors in the last three years.

2. ELECTROCHEMICAL BIOSENSORS

Electrochemical biosensors show high sensitivity and specificity due to the use of biological recognition elements such as enzymes, aptamers, and antibodies [3, 4]. According to the biometric process, they mainly include biocatalytic biosensors and affinity-based biosensors. In the biocatalytic biosensors, electroactive species are produced by exploiting the specific recognition of biological agents such as enzymes, tissue sections, or whole cells. In affinity-based sensors, biological agents such as nucleic acids, antibodies, or receptors are selectively bound to the targets. In addition, the sensitivity, stability, specificity, and conductivity of electrochemical biosensors can be improved by modification of metal nanomaterials on the electrode surface. The high specific surface area of nanomaterials can enhance the biocompatibility and facilitate the immobilization of biomolecules. In recent years, electrochemical biosensors have been widely used in the detection of various analytes due to their high sensitivity, portability, and simple instrumentation.

2.1 Direct detection

For the direct electrochemical detection of biomarkers, antibodies are usually immobilized on the electrode surface. After the capture of the antigens, the electron transfer on the electrode surface will be limited, leading to the change in the electrochemical signal such as potential, impedance, and current (Table 1). Nanomaterials and metal oxides are often used as the electrode modifiers to improve the conductivity and immobilization capacity. Hong et al. developed an electrochemical immunosensor for the detection of AFP by using polydopamine (PDA) nanofilm-modified 3D gold nanowire electrode [5]. The electrode was fabricated by depositing gold nanowires on a bare gold electrode surface for coating the biocompatible PDA. The capture of AFP antigens by the antibodies immobilized on the PDA nanomembrane induced an increase in the impedance. The linear range of the sensor was changed from 0.1 pg/mL to 50 ng/mL, and the detection limit was 0.01 pg/mL. Ordered mesoporous carbon materials have been widely used in energy storage, catalysis, adsorption and other fields due to their good electrical conductivity and large specific surface area. Zhu et al. fabricated a biosensor by immobilizing MnO₂-

functionalized mesoporous carbon hollow spheres (MCHSs) on a glassy carbon electrode [6]. MnO_2 catalyzed the decomposition of hydrogen peroxide to generate an electrochemical signal, and the binding of antibody to AFP resulted in a limited catalytic reaction. The detection limit of this method was found to be 0.03 ng/mL, and the dynamic range was 0.1 ~ 420 ng/mL. Wang et al. developed a label-free electrochemical immunosensor for the detection of AFP using Cu_3Pt nano framework (Cu_3Pt NFS)-modified glassy carbon electrode [7]. Cu_3Pt NFS used as the signal amplifier showed the advantages of large surface area, high catalytic activity and high stability. The linear range of the sensor was in the range of 0.1 ~ 10^4 pg/mL, and the detection limit was 0.033 pg/mL. Chen et al. prepared an immunosensor for AFP detection based on the high catalytic activity of $\text{Cu}_2\text{S}@ \text{Co}_3\text{S}_4$ core-shell isomers for hydrogen peroxide reduction [8]. Due to the large synergistic effect between Cu_2S and Co_3S_4 , $\text{Cu}_2\text{S}@ \text{Co}_3\text{S}_4$ core-shell heterostructures exhibit higher catalytic performance than Cu_2S and Co_3S_4 alone. The biosensor had a wide linear range from 1 pg/mL to 100 ng/mL with a detection limit as low as 0.6 pg/mL. Zhao et al. prepared Cu_2O spherical nanoparticles by hydrothermal reaction, and proposed a signal amplification strategy using the nanocomposites composed of Cu_2O and gold nanoparticles (AuNPs)-modified multi-walled carbon nanotubes (MWCNTs) [9]. Cu_2O exhibited good catalytic performance and redox activity, and AuNPs improved the electron transfer rate and facilitated the immobilization of AFP antibody. Yang et al. constructed a label-free electrochemical sensor for the determination of AFP [10]. The electrode was prepared by immobilization of gold silver platinum nanodendrites on amino-functionalized MoO_2 nanosheets. A detection limit of 3.3 fg/mL for AFP was achieved based on the electrochemical reduction of hydrogen peroxide. A novel electrochemical immunosensor for the detection of AFP was designed based on iron oxide/graphite-phase carbon nitride/silver ($\text{Fe}_3\text{O}_4\text{-g-C}_3\text{N}_4\text{-Ag}$) complex as electrode modifiers by Zhang et al. [11]. The linear range of the sensor was 0.0001 ~ 80 ng/mL, and the detection limit was 0.078 pg/mL.

In addition to nanoparticles and metal oxides, graphene has also been used to modify the sensing electrode because of its good electrical conductivity, stability and biocompatibility [12]. For example, Feng et al. developed a detection platform for AFP detection using hierarchically flower-like gold microstructures/polyaniline/reduced graphene oxide/prussian blue (HFG/PANI/rGO/PB) composite-modified electrode [13]. PANI/rGO could effectively prevented the leakage of PB, and HFG facilitated the immobilization of a large number of antibodies. The linear range of the sensor was 0.01 ~ 30 ng/mL, and the detection limit was 0.003 ng/mL. Dutta et al. designed an efficient immunosensor for AFP detection based on nitrogen-doped graphene quantum dot (N-GQD) and single-walled carbon nanohorns (SWCNHs) (Figure 1) [14]. The N-GQD was decorated on the surface of SWCNHs, and AFP antibody (anti-AFP) was immobilized on the surface of N-GQD@SWCNHs by carbodiimide-mediated coupling reaction. The N-GQD@SWCNHs/anti-AFP provided a good medium for electron transfer and greatly increased the sensitivity of the sensor. The linear range of this method was 0.001 ~ 200 ng/mL with a detection limit of 0.25 pg/mL.

In addition, Li et al. reported a carbon fiber microelectrode (CFME) potentiometric immunosensor [15]. The sensor exhibited a linear range of 0.01 ~ 500 ng/mL with a detection limit of 0.0032 ng/mL. Metal organic frameworks (MOFs) as multifunctional materials with large specific surface area and abundant active sites have been widely used as electrode modifiers.

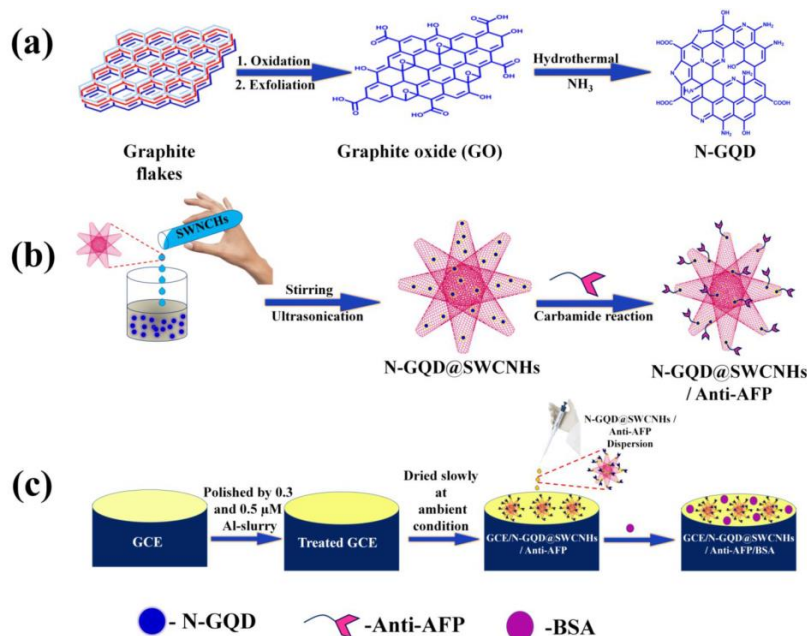


Figure 1. Preparation of GO and N-GQD from graphite flakes (a), preparation of N-GQD decorated SWCNHs nanocomposite (N-GQD@SWCNHs) and anti-AFP incorporated bioconjugates (N-GQD@SWCNHs/anti-AFP) (b), and fabrication procedure of the immunosensor (GCE/N-GQD@SWCNHs/anti-AFP/BSA) (c) [14]. Copyright 2021 American Chemical Society.

Table 1. Analytical performances of various sensing electrodes for AFP detection.

Electrode Modifier	Detection limit (pg/mL)	Linear range (pg/mL)	Ref.
PDA-3D-GEN	0.01	0.1 ~ 5×10 ⁴	[5]
MCHS@MnO ₂	30	100 ~ 4.2×10 ⁵	[6]
Cu ₃ Pt NFs	0.033	0.1 ~ 10 ⁴	[7]
Cu ₂ S@Co ₃ S ₄ @PEI	0.6	1 ~ 1×10 ⁵	[8]
Cu ₂ O/MWCNTs-AuNPs	0.33	1 ~ 4×10 ⁴	[9]
AuAgPtNDs/NH ₂ -MoO ₂ NSs	0.0033	0.1 ~ 1×10 ⁵	[10]
AuNPs/Ag/Fe ₃ O ₄ /g-C ₃ N ₄	0.078	0.1 ~ 8×10 ⁴	[11]
HFG/PANI/rGO/PB	3.0	10 ~ 3×10 ⁴	[13]
N-GQD@SWCNHs	0.25	1 ~ 2×10 ⁵	[14]
anti-AFP	3.2	10 ~ 5×10 ⁵	[15]
FTO/PPy-MO	3.3	10 ~ 1×10 ⁴	[17]

Abbreviation: PDA, polydopamine; PEI, polyethyleneimine; GEN, gold nanowire electrode; MCHS, mesoporous carbon hollow sphere; NFs, nanoframes; MWCNTs, multi-walled carbon nanotubes; AuNPs, gold nanoparticles; AuAgPtNDs; gold silver platinum nanodendrites; g-C₃N₄, graphitic carbon nitrides; HFG, hierarchically flower-like gold microstructures; PANI, polyaniline; rGO, reduced graphene oxide; P, prussian blue; FTO, fluorine-doped tin oxide; PPy, polymerized polypyrrole; MO, methyl orange.

Gu et al. reported a method for the controlled synthesis of Co-doped MIL-96, and constructed a sensing platform to achieve highly sensitive detection of AFP [16]. Taheri et al. prepared an electrochemical impedance sensor for the detection of carcinoembryonic antigen (CEA) and AFP based on a high-performance sensing layer of dual-template molecularly imprinted polymer (DMIP) [17]. The sensor exhibited good linearity for AFP at the concentration ranged from 10 to 10^4 ng/mL, and showed a detection limit of 3.3 ng/mL.

2.2 Sandwich-type detection

Sandwich-type biosensors usually consist of a recognition unit such as capture antibody (Ab_1) immobilized on the electrode, and a signal probe (e.g., enzyme or redox label) conjugated with the detection antibody (Ab_2). Signal amplification is the general strategy to improve the detection sensitivity of sandwich-type biosensors. Nanomaterials, polymer/nanomaterial composites, metal oxides, and carbon materials are the commonly used amplifiers in electrochemical immunosensors (Table 2). Among them, gold and silver nanoparticles are the two most commonly used nanomaterials. They have unique optical, electrical and chemical properties and show a wide application field [18]. Tan et al. developed a sandwich-type sensor for AFP detection based on PdAg nanodendrites-modified CoFe prussian blue (PdAg NDs/CoFe PBA) as the signal probe [19]. The unique steric structure of CoFe PBA enabled the exposure of active sites and atomic positions, thereby amplifying the electrochemical signal. PdAg NDs have good catalytic activity and facilitate the immobilization of a large number of antibodies through Pd-N and Ag-N bonds. When Ab_2 was bound to AFP antigen, PdAg NDs catalyzed the reduction of H_2O_2 to generate an electrical signal. The linear range of the sensor was 100 fg/mL ~ 200 ng/mL, and the detection limit was 18.6 fg/mL. Zhang et al. designed an immunosensor with FeS_2 -AuNPs as HRP-mimic enzymes and nickel hexacyanoferrate nanoparticles (NiHCFNPs) as the signal probes [20]. First, AuNPs were electrodeposited on the surface of glassy carbon electrode, and then electroactive NiHCFNPs were modified on the electrode for the assembly of anti-AFP (Ab_1). The Ab_2 -labeled FeS_2 -AuNPs anchored by the captured AFP catalyzed the oxidation of 4-chloro-1-naphthol (4-CN) to generate extensive precipitates on the electrode surface. The precipitates caused the decrease in the electrochemical signal, thus achieving the quantitative detection of AFP. Xiao et al. developed a sandwich-type electrochemical immunosensing platform by modifying the electrode with rGO-tetraethylene pentamine (rGO-TEPA-Thi-Au) with thionine (Thi) and AuNPs for the immobilization of Ab_1 [21]. AuPt binary nanoparticles were used to modify the ordered mesoporous carbon (CMK-3) as the signal probes, which can effectively catalyze the reduction of hydrogen peroxide. The linear range of the sensor was 0.005 ~ 100 ng/mL, and the detection limit was 0.0022 ng/mL. Rong et al. reported an ultrasensitive platform for immunoassay of AFP using the composite of ordered mesoporous carbon (OMC) and AuNPs (OMC@AuNPs) [22]. The OMC@AuNPs-modified carbon electrode was beneficial to the immobilization of Ab_1 and facilitated the electron transfer. Ab_2 was modified on AuPt-methylene blue (AuPt-MB), a redox-active species with good biocompatibility and conductivity. Quantitative analysis of AFP was achieved by monitoring the electrochemical reduction of MB. Sun et al. constructed a sensing platform for AFP detection by depositing AuPt-doped vertical graphene on glassy carbon electrode [23]. The signal probe was obtained by immobilizing Ab_2 on carbon nanotubes modified with

gold and methyl orange (MO). A wide linear range from 1 fg/mL to 100 ng/mL was obtained based on the change of electrochemical signal from MO. Meng et al. developed a sandwich-type sensing platform with AuNPs-functionalized silica microspheres as the electrode modifiers [24]. In this study, adriamycin (ADM) was used as the signal label.

In recent years, some polymer/nanomaterial composites have also been employed to anchor the capture antibody because they have good biocompatibility and abundant sites for the modification of signal molecules. For example, Liang et al. designed an electrochemical biosensor for AFP detection using poly(2-hydroxyethyl methacrylate) (PHEMA)/graphene oxide (GO) nanocomposites [25]. The hydroxyl functional groups on the surface of PHEMA allowed for the modification of a large number of signal molecules, thus significantly amplifying the signal of electrochemical biosensor. AFP antibody (Ab_1) was immobilized on AuNPs and rGO-modified glassy carbon electrode to capture AFP. The linear range of the sensor by square wave voltammetry was 0.0025~25 ng/mL with a detection limit of 0.403 pg/mL. Polydopamine (PDA) is a type of multifunctional biomimetic materials with good biocompatibility. Wang et al. developed a highly selective biosensor by immobilizing the recognition element of Ab_2 and electroactive redox probe of aminoferrocene (AF) on PDA nanospheres (Figure 2) [26]. The catechol/quinone moieties in PDA facilitated the immobilization of antibody and improved the electrochemical performance. The electrochemical signal was first amplified by the Ab_2 -PDA-AF signal tag, and then the attached AF/ AF^+ reacted with the catechol groups of PDA nanospheres to further amplify the signal. This immunosensor exhibits good selectivity, stability, and reproducibility, and has good applicability in human serum samples with a detection limit of 0.01 pg/mL. Polyaniline (PANI) is one of the commonly used conductive polymers in the field of electrochemical biosensors due to its excellent transduction ability and biocompatibility. Amarnath et al. developed an electrochemical biosensor for the detection of AFP by modifying the electrode with PANI and silver nanoparticles/bovine serum albumin [27]. The signal probe was prepared by conjugation of horseradish peroxidase/secondary antibody (HRP- Ab_2) on silver nanoparticles, and the redox reaction between H_2O_2 and hydroquinone (HQ) was catalyzed by HRP to generate an electrochemical signal. The detection limit of the sensor for AFP detection was 4.7 pg/mL. Furthermore, Anbalagan et al. synthesized carboxylic acid-tethered polyaniline (PCOOH) by covalent functionalization of the PANI backbone with thiols-contained carboxylic acid groups, which improved the efficiency of antibody immobilization [28]. The capture antibody (Ab_1) was immobilized on the PCOOH-modified glassy carbon electrode to capture the AFP antigen. A low detection limit of 2 pg/mL was obtained by using HRP-labeled secondary antibody (Ab_2) as the signal probe to catalyze the H_2O_2 /HQ redox reaction. Zhao et al. developed an immunosensor based on a polymer brush/GO probe [29]. Polymer brush-based composites (poly (vinyltetrazole-co-hydroxyethyl methacrylate)-g-GO, P(VT-co-HEMA)-g-GO) were synthesized by surface-initiated atom transfer radical polymerization (SI-ATRP) and click chemistry technique. The immunosensor showed a wide detection range from 25 pg/mL to 5×10^4 pg/mL and a low detection limit of 0.183 pg/mL.

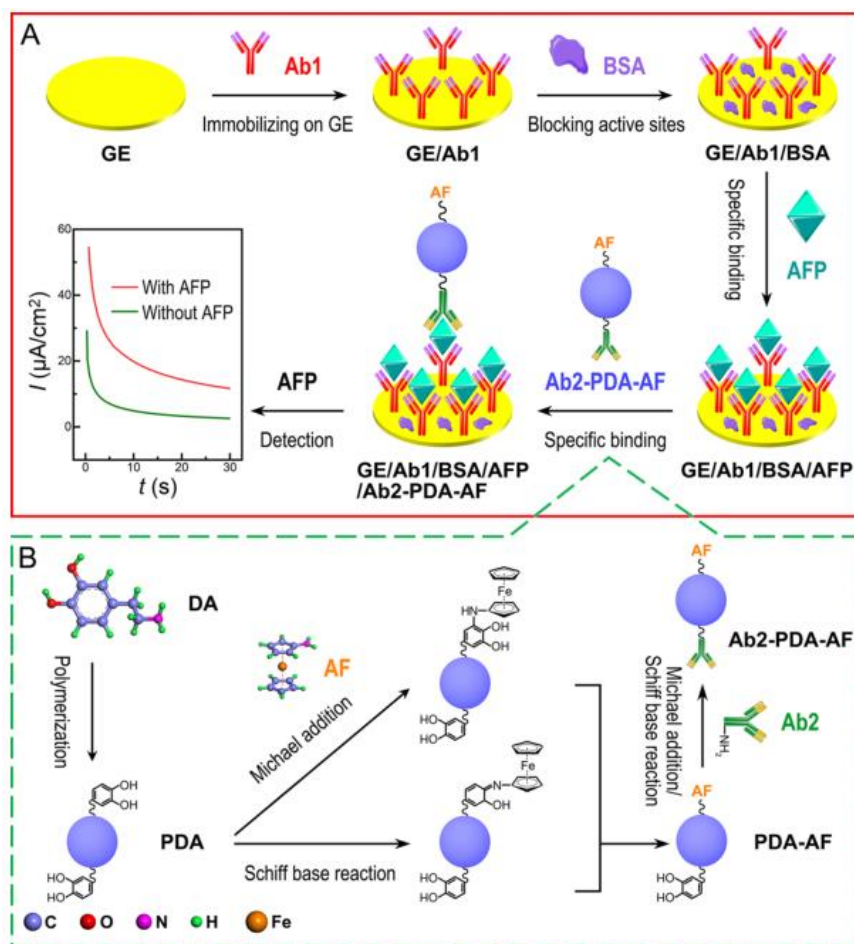


Figure 2. (A) Schematic illustration for the construction and function of the immunosensor employing multifunctional Ab₂-PDA-AF nanolabel, including immobilizing Ab₁ on GE, BSA blocking active sites, selective binding of AFP to GE/Ab₁/BSA, specific binding of Ab₂-PDA-AF to GE/Ab₁/BSA/AFP, and AFP detection by chronoamperometric measurements of GE/Ab₁/BSA/AFP/Ab₂-PDA-AF; (B) Preparation of the Ab₂-PDA-AF nanolabel, including fabrication of PDA nanospheres, AF-modified PDA nanospheres (PDA-AF), and the final Anti-AFP detection antibody and AF dual-functioned nanolabel (Ab₂-PDA-AF) [26]. Copyright 2021 American Chemical Society.

Furthermore, Lv et al. reported a gas-based electrochemical biosensor for AFP detection (Figure 3) [30]. This electrochemical biosensor realized the separation of sensing interface and molecular assembly. It effectively avoids the biological assembly process at the sensing interface, thereby ensuring the stability and reproducibility of the analysis results. The detection antibody was coupled to dendritic Pt nanoparticles (DPNs) to form a sandwich-type sensor. The signal came from the chemical signal transduction between H₂ and Pd nanowires at the double-layer immunosensing interface. In this work, H₂ as a bridge was originated from DPNs to catalyze NH₃BH₃ and produce an electrical signal by reaction with Pd nanowires. However, oxygen adsorbed on the surface of Pd nanostructures limited the adsorption of H₂ and reduced the signal transduction. To solve this problem, ZIF-67 was used as a molecular sieve to intercept oxygen. The dynamic range of this electrochemical sensor is 0.1 ~ 50 ng/mL, and the detection limit is 0.04 ng/mL. Li et al. developed a portable personal glucometer for AFP

detection using antibody-invertase cross-linkage nanoparticles as the signal tags [31]. Nanotags were prepared by the reverse micellar method with glutaraldehyde as the linker. The capture antibody immobilized on the microplate was bound with the antigen to form a sandwich-type reaction pattern. Due to the introduction of invertase, sucrose was hydrolyzed into glucose and fructose, and the resulting glucose was measured by a portable personal glucometer. The concentration of detectable glucose increased with the increase of AFP concentration.

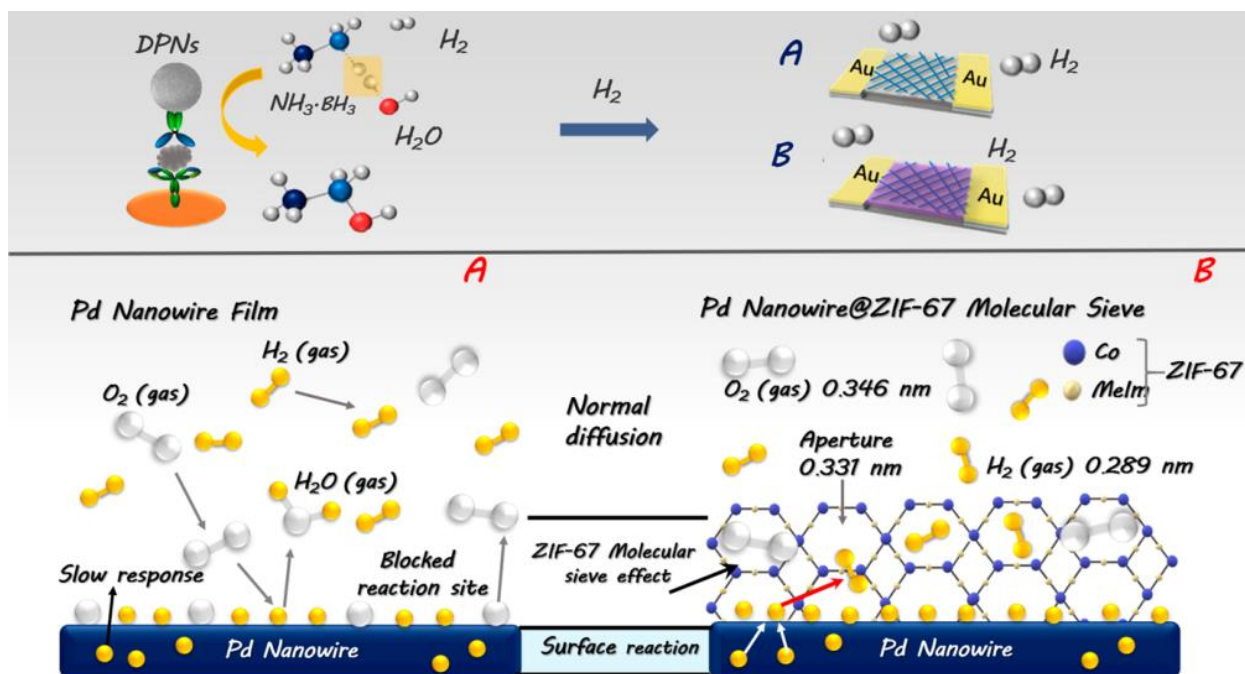


Figure 3. Illustration of H₂-based electrochemical biosensor with Pd nanowires@ZIF-67 molecular sieve bilayered sensing interfaces: (A) interaction between Pd Nanowires and H₂ under O₂ interference. (B) Self-assembly ZIF-67 on surface of Pd nanowires films as molecular sieve excluding O₂ interference [30]. Copyright 2019 American Chemical Society.

Traditional sandwich-type biosensors are usually only able to detect a single tumor biomarker because the simultaneous detection of multiple markers may cause the signal interference. The biosensor for single biomarker may greatly limit the improvement of detection efficiency. Therefore, the strategy for determining multiple cancer biomarkers has attracted great attention. For example, Li et al. developed a multiple immunosensor for simultaneous detection of three biomarkers including AFP, prostate specific antigen (PSA) and carcinoembryonic antigen (CEA) based on metal ion (Pb²⁺, Cd²⁺, Zn²⁺)-functionalized nanocomplexes as the immune probes [32]. The CNSs@AuNPs nanocomposites were produced by electrostatic assembly of carbon nanospheres CNSs and AuNPs, and the secondary antibody was subsequently assembled on the CNSs@AuNPs. The sensor electrodes were fabricated by immobilizing primary antibodies onto the AuNPs-modified glassy carbon electrode. In this study, the sensor can be used to detect multiple analytes simultaneously with three distinguishable square wave voltammetry (SWV) signal peaks. AFP in the concentration range of 0.01-80 ng/mL was readily determined with a detection limit of 2.6 pg/mL. Filik et al. developed a novel sandwich sensor by

immobilizing ethylenediamine-MWCNT aerogels (EDA-CAGs), gold nanoparticles, and capture antibody on screen-printed electrodes (SPCE) [33].

Table 2. Analytical performances of sandwich biosensors for AFP detection.

Signal label	Detection limit (fg/mL)	Linear range (ng/mL)	Ref.
PdAg NDs/CoFe/PBA	0.0186	$1 \times 10^{-4} \sim 200$	[19]
FeS ₂ -AuNPs	0.028	$1 \times 10^{-4} \sim 100$	[20]
CMK-3@AuPtNPs	2.2	0.005 ~ 100	[21]
AuPt-MB	3.33	$1 \times 10^{-5} \sim 100$	[22]
MO/CNT-Au	0.7	$1 \times 10^{-6} \sim 100$	[23]
ADM@AuNPs@SiO ₂	1.7×10^2	$5 \times 10^{-4} \sim 75$	[24]
PHEMA/GO	4.03×10^2	0.0025 ~ 25	[25]
PDA-AF	10	0.0005 ~ 1	[26]
AgNPs-HRP	4.7×10^3	1 ~ 10	[27]
HRP	2×10^3	0.25 ~ 40	[28]
P(VT-co-HEMA)-g-GO	1.83×10^2	0.0025 ~ 50	[29]
DPNs	4×10^4	0.1 ~ 50	[30]
pAb ₂ -IVT NPs	5.4×10^3	0.01 ~ 300	[31]
CNSs@AuNPs@Pb	2.6×10^3	0.01 ~ 80	[32]
AuNP-EDA-CAGs	1.5×10^3	0.005 ~ 1	[33]
PdAgCeO ₂ MNS	1×10^3	0.005 ~ 100	[34]
PDA/rGO-PEI	83	$1.17 \times 10^{-4} \sim 117$	[35]
PSMA-Fc/GO	14	$3.5 \times 10^{-4} \sim 35$	[36]
CdS	1.1×10^2	$1 \times 10^{-3} \sim 10$	[37]

Abbreviation: PdAg NDs, PdAg nanodendrites; PBA, prussian blue analog; CMK-3, ordered mesoporous carbon; AuPtNPs, AuPt binary nanoparticles; MB, methylene blue; MO, methyl orange; CNT, carbon nanotubes; ADM, Adriamycin; PHEMA, poly(2-hydroxyethyl methacrylate); GO, graphene oxide; PDA, polydopamine; AF, aminoferrocene; HRP, horseradish peroxidase; P(VT-co-HEMA)-g-GO, poly(vinyltetrazole-co-hydroxyethyl methacrylate)-g-GO; CNSs, carbon nanospheres; EDA-CAGs, ethylenediamine-MWCNT aerogels; MNS, mesoporous nanospheres; rGO, reduced graphene oxide; PEI, polyethyleneimine; PSMA, Poly(styrene-alt-maleic anhydride); Fc, ferrocenecarboxylic acid; DPNs, dendritic Pt nanoparticles; pAb₂-IVT NPs, antibody-invertase nanoparticles.

Meanwhile, AuNP-functionalized EDA-CAGs were used as the signal tags to label the detection antibody. The sensor can be used to detect both AFP and CEA targets simultaneously. In addition, Hong's group reported an immunoassay platform for the detection of two targets [34]. A sandwich immunosensor was constructed by labeling of carcinoembryonic antigen (CEA) with PdAgCeO₂ mesoporous nanospheres (PdAgCeO₂ MNS) and labeling of AFP with MnO₂ nanosheets. Both PdAgCeO₂ MNS and MnO₂ exhibited excellent catalytic performance for hydrogen peroxide. More interestingly, they found that ascorbic acid (AA) even at a low concentration could reduce MnO₂ into Mn²⁺, which made MnO₂ lose its catalytic activity for hydrogen peroxide reduction. Therefore, AA can act as a "switch" to quickly decrease the catalytic ability of MnO₂. Without AA, the signal was caused by the two antigens of CEA and AFP, but it was originated from CEA only without the addition of AA. Zhao et al. constructed a novel multi-signal amplification electrochemical immunoassay platform for

simultaneous detection of three tumor biomarkers [35]. The platform was successfully developed based on polyethyleneimine (PEI)-PDA/rGO nanocomposites. PDA/rGO was used to load both detection antibody (Ab_2) and PEI. Meanwhile, PEI was also used to load different signal labels, including ferrocenecarboxylic acid (Fc), anthraquinone-2-carboxylic acid (Aq) and acetylsalicylic acid (ASA). The electrochemical performances of the designed sandwich immunosensor were successfully investigated by cyclic voltammetry (CV) and differential pulse voltammetry (DPV). In addition, Wang et al. develop an electrochemical immunosensor for the simultaneous detection of three tumor markers, AFP, PSA and carbohydrate antigen 125 (CA 125) using Fc, Aq and ASA as the signal markers [36]. Fc, Aq, and ASA-labeled poly(styrene-alt-maleic anhydride) (PSMA) were loaded into diethylenetriamine-modified GO (GO-DETA) as the signal probe. Then, gold nanoparticles and rGO-modified glassy carbon electrode were used as the working electrode. The detection limit of this method for AFP detection was 14 fg/mL, and the dynamic range was 0.35 pg/mL ~ 35 ng/mL. Yu et al. developed a ratiometric electrochemical biosensor using metal sulfide nanoparticles as the signal labels for the detection of multiple cancer markers [37]. Metal sulfide (ZnS, CdS, PbS or HgS) nanoparticles were used as the distinguishable signal tags, and AFP, CEA, CA125 and CA19-9 were determined as the model target antigens. After immunorecognition, the signal tags in the sandwich immune complexes were dissolved in a mixture of hydrogen peroxide and hydrochloric acid. Indirect measurement of the biomarkers was achieved by measuring the concentrations of Hg(II), Pb(II) and Zn(II) using differential pulse anodic stripping voltammetry (DPASV).

2.3 Aptasensors

Aptamers are usually oligonucleotides (DNA or RNA) screened by SELEX technology. They exhibit high affinity and specificity for various targets such as proteins, peptides, nucleic acids, viruses, and even cells and tissues [38]. Due to the advantages of simple synthesis, high stability, diverse design, convenient modification and low cost, aptamers are often used as the identification probes to construct biosensors in combination with different transduction technologies. The development of an efficient aptasensor is dependent upon the design of electrochemical platform. Carbon materials (graphene, carbon nanotubes, etc.) as electrode materials exhibit various advantages, including good mechanical property, large specific surface, easy functionalization, and excellent biocompatibility, which make them suitable for sensing applications with satisfactory results. Therefore, carbon materials have been widely used in the field of aptasensors. Carbon materials-based AFP aptasensors have been developed in recent years. For example, Zhang et al. developed an aptamer-based sensing platform for the detection of AFP based on graphene oxide-modified gold electrode [39]. Due to the limitation of space, an aptamer can only be bound to one target, but it is not conducive to the signal amplification of biosensor. For this view, prussian blue nanoparticles (PBNPs) with unique electrochemical signal were used as the signal-generating tags to label AFP aptamer by covalent coupling reaction. The aptamer-PBNP composites were modified on the GO-modified gold electrode. When AFP was added, a number of PBNP-aptamer conjugates were dissociated from the electrode, resulting in a significant decrease in the DPV signal. The linear range of the sensor was 0.01 ~ 300 ng/mL, and the detection line was 6.3 pg/mL. Moreover, a label-free aptasensor for the detection of AFP was designed by Li et al. [40]. In this study, gold-

platinum metallic nanoparticles and rGO/chitosan/ferrocene nanohybrids-modified SPEC were used to immobilize the AFP aptamers. After the addition of AFP, the AFP-aptamer conjugate was formed on the sensing surface, resulting in an increase in the impedance and a decrease in the peak current of redox probe. The dynamic range of this method for AFP detection was 0.001 ~ 10.0 mg/mL, and a detection limit of 0.3013 ng/mL was achieved. Rahmati et al. developed an electrochemical aptasensor based on nanoboxes as the substrates for AFP detection [41]. The sensing platform was formed by immobilization of Ni(OH)₂ nanosheets on the hollow nitrogen-doped carbon nanoboxes, which showed excellent electrical conductivity, stability and abundant AFP-binding sites. The performances of the sensor were investigated by electrochemical impedance spectroscopy. The AFP content was linearly related to charge transfer resistance from 1 fg/mL to 100 ng/mL, and a low detection limit of 0.3 fg/mL was obtained. Upan et al. developed an aptamer sensing platform based on Pt nanoparticles and carboxylated GO-modified screen-printed graphene-carbon paste electrode (SPGE) [42]. The linear range of the sensor was 3 ~ 30 ng/mL, and the detection limit was 1.22 ng/mL. In addition, Huang et al. developed a low-cost AFP aptasensor by extracting nitrogen-doped mesoporous carbon nanomaterials from plant biomass [43]. With biomass carbon as the immobilization matrix for AFP aptamer, the method showed the advantages of environmental friendliness, low-cost and good electrochemical performance.

In addition to carbon materials, metal nanomaterials, polymer materials and metal-organic frameworks (MOFs) also have a wide range of applications in the field of electrochemical sensors. Gu et al. prepared an electrochemical aptasensor for AFP detection based on MIL-96 modified electrode [44]. The controllable synthesis of MIL-96 was realized with copper ions as the precursors. In addition, copper ions can change the morphology of MOFs and increase the conductivity, which is beneficial to improve the sensitivity of the sensor.

Light-addressable potentiometric sensor (LAPS) is a potentiometric electrochemical sensor based on the semiconductor field effect principle, which can monitor the biochemical reactions on the LAPS chip through the change of potential. Li et al. reported an aptamer-based sensing strategy for AFP detection based on gold nanoparticles-functionalized LAPS [45]. AFP aptamer as a recognition element was attached to the surface of LAPS after the silanization treatment. The AFP target captured by the aptamer caused a potential change, thus realizing the quantitative analysis of AFP. Han et al. designed a sandwich-type aptasensor [46]. The AFP aptamer was immobilized on the gold electrode to selectively capture the target, and then the captured AFP was interacted with the probe DNA to form an aptamer/AFP/DNA sandwich structure on the electrode surface. The massive accumulation of methylene blue-labeled probe DNA on the electrode surface caused the amplification of the electrical signal. Hydrogel materials with large specific surface area and good biocompatibility can also be used to develop sensitive electrochemical biosensing platform. For example, Li et al. developed an electrochemical aptasensor for ultrasensitive detection of AFP based on guanosine-based G4 hydrogel [47]. The transparent hydrogel (G-PyB/KCl hydrogel) was prepared by mixing guanosine (G), pyridine-4-boronic acid (PyB) and aqueous KCl in a molar ratio of 1:1:1. The resulting G-PyB/KCl hydrogel was immobilized on a bare gold electrode to provide high electrical conductivity and 3D microenvironment favorable for the immobilization of ligands. When the target AFP was added, the binding of the aptamer to the AFP produced a detectable electrical signal. In addition to increasing the sensitivity of the sensing platform, the anti-fouling of the reaction interface is also an important issue that needs to be noticed

[48]. For example, false positive reaction caused by non-specific adsorption and low loading efficiency may limit the sensitivity, and thus the clinical applications of biosensors are still faced with many challenges. To this end, Liu et al. developed a low-contamination electrochemical sensing platform with a zwitterionic peptide-based layered structure for highly sensitive detection of AFP [49]. Hierarchical antifouling peptide brushes formed by conjugation of CPPPPEKEKEKEK (Pep4) with CPPPPEKEKEKEK (Pep3) were subsequently immobilized on the electrode surface and then functionalized with AFP aptamer. The sensor had excellent anti-fouling ability and high sensitivity even in the presence of high concentration of non-specific proteins. It showed a linear range from 1 fg/mL to 1 ng/mL with a low detection limit of 0.59 fg/mL. Zhao et al. suggested that the peptide with isomer D-Amino acids (cppPPEKEKEKEKek) showed a strong anti-fouling ability and high stability [50]. An electrochemical sensor was constructed by coupling of conductive polymer polyaniline and polypeptide on the electrode surface, realizing the accurate detection of AFP in clinical samples with a detection limit down to 0.03 fg/mL.

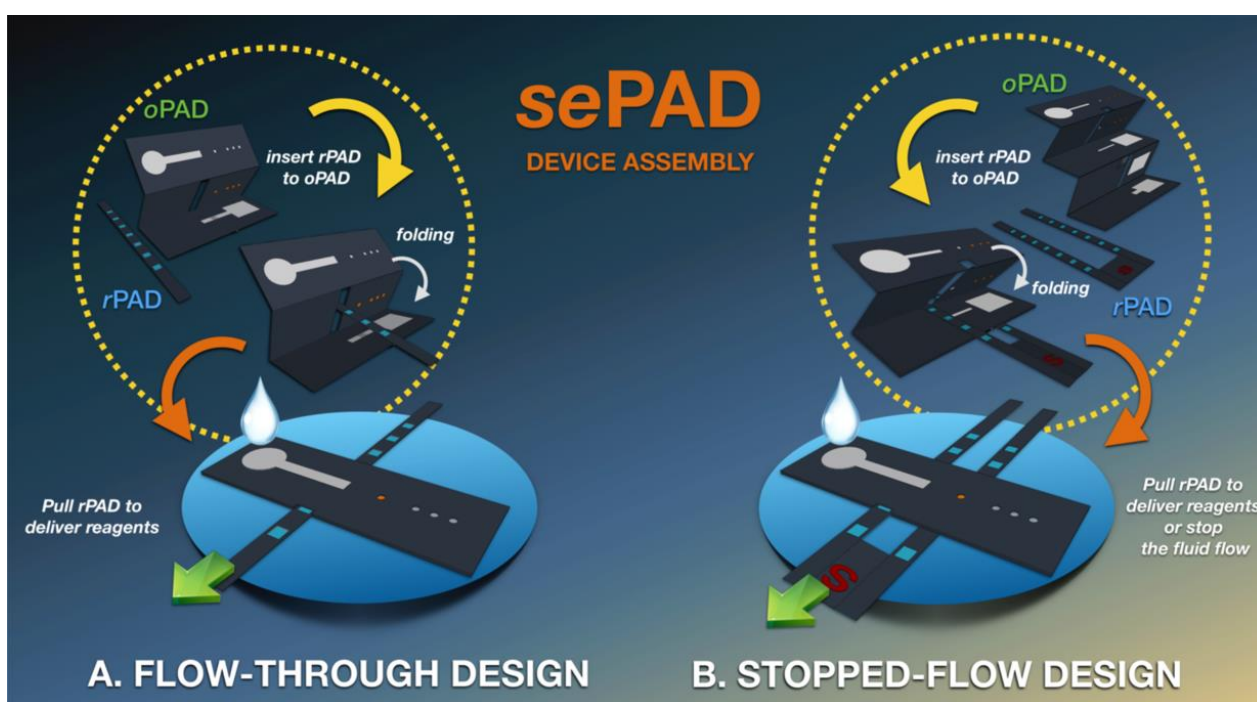


Figure 4. Schematic illustration of the sePAD components and device assembly using (A) flow-through design and (B) stopped-flow design [51]. Copyright 2019 American Chemical Society.

2.4 Others

Paper-based microfluidic immunochips can be used to develop immunosensing platforms due to their high sensitivity, low cost, and easy miniaturization. Yakoh et al. reported a 3D capillary-driven paper-based microfluidic device for AFP detection (Figure 4) [51]. The device consists of an origami folding paper (oPAD) and a moving reagent-stored pad (rPAD) in which the detected sample was stored and moved in turn to the detection zone on the oPAD. The electrode was decorated with GO nanosheets, and AFP was captured by the immobilized AFP antibody as a recognition element. After the formation

of antigen-antibody complex, the interface electron transfer was hindered with $\text{Fe}(\text{CN})_6^{3-/4-}$ as the redox probe, which caused the increase of electrochemical impedance. In addition, Hu et al. designed an ultrasensitive electrochemical immunochip based on MoS_2/PDDA hybrid thin film using a hierarchical self-assembly method [52]. The three-electrode system was integrated into the microchannel and electrochemical impedance spectroscopy was used to monitor the change of AFP concentration. The MoS_2/PDDA -functionalized electrode had excellent biocompatibility and conductivity, which could promote the binding of AFP antibody to AFP. The linear range of the sensor was 0.1 ~ 10 ng/mL, and the detection limit was 0.033 ng/mL by electrochemical impedance spectroscopy.

3. CONCLUSION

Electrochemical biosensors have been developed to detect AFP with high simplicity, sensitivity and selectivity. In the future, the development of electrochemical biosensors may be mainly carried out in the following aspects: the detection of complex biological samples such as cancer cells and blood, the use of novel nanomaterials for signal amplification, designing of new sensing modes to improve the repeatability, practicability and sensitivity, and a miniaturized, portable and cheap electrochemical device for real-time analysis. We believe that the electrochemical AFP biosensor will be put into practical application as soon as possible and play a more and more important role in the early diagnosis and postoperative healing of patients with liver cancer.

ACKNOWLEDGMENTS

This work was supported by the Scientific Research Fund of Hunan Provincial Education Department (21B0923).

References

1. A. Mohammadinejad, R. Kazemi Oskuee, R. Eivazzadeh-Keihan, M. Rezayi, B. Baradaran, A. Maleki, M. Hashemzaei, A. Mokhtarzadeh and M. de la Guardia, *TrAC-Trend. Anal. Chem.*, 130 (2020) 115961.
2. T. Sun, Y. Guo and F. Zhao, *Int. J. Electrochem. Sci.*, 16 (2021) 210732.
3. N. Xia, Y. Huang, Y. Zhao, F. Wang, L. Liu and Z. Sun, *Sens. Actuat. B: Chem.*, 325 (2020) 128777.
4. N. Xia, D. Wu, T. Sun, Y. Wang, X. Ren, F. Zhao, L. Liu and X. Yi, *Sens. Actuat. B: Chem.*, 327 (2021) 128913.
5. Y. Hong, Y. Wang and Y. Zhu, *Electrochim. Acta*, 364 (2020) 137328.
6. X. Zhu, Y. Dai, Y. Sun, H. Liu, W. Sun, Y. Lin, D. Gao, R. Han, X. Wang and C. Luo, *Mater. Sci. Eng. C: Mater. Biol. Appl.*, 107 (2020) 110206.
7. A.-J. Wang, X.-Y. Zhu, Y. Chen, P.-X. Yuan, X. Luo and J.-J. Feng, *Sens. Actuat. B: Chem.*, 288 (2019) 721.
8. H. Chen, J. Cai, J. Yang, Z. Zhong, M. Ma, W. Deng, Y. Tan and Q. Xie, *Sens. Actuat. B: Chem.*, 348 (2021) 130703.
9. C. Zhao, K. Cao, C. Ma, W. Li, Y. Song, X. Qiao and C. Hong, *Micro Nano Lett.*, 15 (2020) 125-129.

10. Q. Yang, P. Wang, F. Tang, S. Wang, Z. Zhao, Y. Wang, Y. Li, Q. Liu and Y. Dong, *J. Electrochem. Soc.*, 168 (2021) 057506.
11. M. M. Zhang, K. H. Cao, L. S. Mei, X. Wang, X. C. Liao, X. W. Qiao and C. L. Hong, *Chemistryselect*, 6 (2021) 3394.
12. D. Deng, Y. Hao, S. Yang, Q. Han, L. Liu, Y. Xiang, F. Tu and N. Xia, *Sens. Actuat. B. Chem.*, 286 (2019) 415.
13. D. Feng, K. Zhang, Y. Lu, J. Chen and Y. Wei, *Anal. Sci.*, 36 (2020) 1501.
14. K. Dutta, S. De, B. Das, S. Bera, B. Guria, M. S. Ali and D. Chattopadhyay, *ACS Biomater. Sci. Eng.*, 7 (2021) 5541.
15. L. Li, D. Liang, W. Guo, D. Tang and Y. Zeng, *Electroanalysis*, 33 (2021) 1.
16. C. Gu, J. Li, G. Yang, L. Zhang, C.-S. Liu and H. Pang, *Chin. Chem. Lett.*, 31 (2020) 2263.
17. N. Taheri, H. Khoshshafar, M. Ghanei, A. Ghazvini and H. Bagheri, *Talanta*, 239 (2022) 123146.
18. Y. Chang, X. Ma, T. Sun, L. Liu and Y. Hao, *Talanta*, 234 (2021) 122649.
19. M. Tan, C. Zhang, Y. Li, Z. Xu, S. Wang, Q. Liu and Y. Li, *Bioelectrochemistry*, 145 (2022) 108080.
20. L. Zhang, X. Xie, Y. Yuan, Y. Chai and R. Yuan, *Electroanalysis*, 31 (2019) 1019.
21. H. Xiao, S. Wei, M. Gu, Z. Chen and L. Cao, *Microchem. J.*, 170 (2021) 106641.
22. S. Rong, L. Zou, Y. Li, Y. Guan, H. Guan, Z. Zhang, Y. Zhang, H. Gao, H. Yu, F. Zhao, H. Pan and D. Chang, *Bioelectrochemistry*, 141 (2021) 107846.
23. D. Sun, H. Li, M. Li, C. Li, L. Qian and B. Yang, *Biosens. Bioelectron.*, 132 (2019) 68-75.
24. W. Meng, M. Li and Y. Zhang, *Anal. Methods*, 13 (2021) 2665.
25. Y. Liang, X. Zhao, N. Wang, J. Wang, H. Chen, L. Bai and W. Wang, *RSC Advances*, 9 (2019) 17187.
26. Y. Wang, Y. Hong, M. Wang and Y. Zhu, *ACS Appl. Nano Mater.*, 5 (2021) 1588.
27. C. A. Amarnath and S. N. Sawant, *Electroanalysis*, 32 (2020) 2415.
28. A. Chellachamy Anbalagan and S. N. Sawant, *Microchim. Acta*, 188 (2021) 403.
29. X. Zhao, N. Wang, H. Chen, L. Bai, H. Xu, W. Wang, H. Yang, D. Wei, L. Yang and Z. Cheng, *Polym. Chem.*, 11 (2020) 900.
30. S. Lv, K. Zhang, L. Zhu, D. Tang, R. Niessner and D. Knopp, *Anal. Chem.*, 91 (2019) 12055.
31. L. Li, D. Liang, W. Guo, D. Tang and Y. Zeng, *Electroanalysis*, 34 (2021) 246.
32. L. Li, Y. Wei, S. Zhang, X. Chen, T. Shao and D. Feng, *J. Electroanal. Chem.*, 880 (2021) 114882.
33. H. Filik, A. A. Avan, N. Altaş Puntar, M. Özyürek, Z. B. Güngör, M. Kucur, H. Kemiş and D. A. Dicle, *J. Electroanal. Chem.*, 900 (2021) 115700.
34. W. Li, Y. Yang, C. Ma, Y. Song, X. Qiao and C. Hong, *Talanta*, 219 (2020) 121322.
35. X. Zhao, J. Wang, H. Chen, H. Xu, L. Bai, W. Wang, H. Yang, D. Wei and B. Yuan, *Sens. Actuat. B: Chem.*, 301 (2019) 127071.
36. N. Wang, J. Wang, X. Zhao, H. Chen, H. Xu, L. Bai, W. Wang, H. Yang, D. Wei and B. Yuan, *Talanta*, 226 (2021) 122133.
37. L. Yu, X. Cui, H. Li, J. Lu, Q. Kang and D. Shen, *Analyst*, 144 (2019) 4073.
38. X. Ma, *Int. J. Electrochem. Sci.*, 15 (2020) 7663.
39. B. Zhang, H. Ding, Q. Chen, T. Wang and K. Zhang, *Analyst*, 144 (2019) 4858.
40. W. Li, M. Chen, J. Liang, C. Lu, M. Zhang, F. Hu, Z. Zhou and G. Li, *Anal. Methods*, 12 (2020) 4956.
41. Z. Rahmati, M. Roushani and H. Hosseini, *Talanta*, 237 (2022) 122924.
42. J. Upan, N. Youngvises, A. Tuantranont, C. Karuwan, P. Banet, P. H. Aubert and J. Jakmunee, *Sci. Rep.*, 11 (2021) 13969.
43. X. Huang, B. Cui, Y. Ma, X. Yan, L. Xia, N. Zhou, M. Wang, L. He and Z. Zhang, *Anal. Chim. Acta*, 1078 (2019) 125.
44. C. Gu, Y. Peng, J. Li, C.-S. Liu and H. Pang, *Appl. Mater. Today*, 20 (2020) 100745.

45. G. Li, W. Li, S. Li, X. Shi, J. Liang, J. Lai and Z. Zhou, *Biochem. Engin. J.*, 164 (2020) 107780.
46. B. Han, L. Dong, L. Li, L. Sha, Y. Cao and J. Zhao, *Sens. Actuat. B: Chem.*, 325 (2020) 128762.
47. J. Li, H. Wei, Y. Peng, L. Geng, L. Zhu, X. Y. Cao, C. S. Liu and H. Pang, *Chem. Commun.*, 55 (2019) 7922.
48. C. Jiang, G. Wang, R. Hein, N. Liu, X. Luo and J. J. Davis, *Chem. Rev.*, 120 (2020) 3852.
49. N. Liu, X. Fan, H. Hou, F. Gao and X. Luo, *Anal. Chim. Acta*, 1146 (2021) 17.
50. S. Zhao, N. Liu, W. Wang, Z. Xu, Y. Wu and X. Luo, *Biosens. Bioelectron.*, 190 (2021) 113466.
51. A. Yakoh, S. Chaiyo, W. Siangproh and O. Chailapakul, *ACS Sens.*, 4 (2019) 1211.
52. T. Hu, M. Zhang, Z. Wang, K. Chen, X. Li and Z. Ni, *Microchem. J.*, 158 (2020) 105209.

© 2022 The Authors. Published by ESG (www.electrochemsci.org). This article is an open access article distributed under the terms and conditions of the Creative Commons Attribution license (<http://creativecommons.org/licenses/by/4.0/>).